JOURNAL OF SOLID STATE CHEMISTRY 120, 128–136 (1995)

Oxide Ion Conduction in Solid Solutions $Ln_{1-x}Sr_xCoO_{3-\delta}$ (Ln = La, Pr, Nd)

V. V. Kharton, E. N. Naumovich, A. A. Vecher, and A. V. Nikolaev

Institute of Physico-Chemical Problems, Belarus State University, 14 Leningradsky Str., 220080, Minsk, Republic of Belarus

Received July 26, 1994; in revised form May 30, 1995; accepted June 7, 1995

Ln(Sr)$CoO_{3-\delta}$ (Ln = La, Pr, Nd) solid solutions as high-temperature mixed ion and electron conductors are described. Electrical conductivity and oxygen permeability as function of temperature and oxygen partial pressure were measured. A model for the oxygen flow density through the mixed conductor caused by chemical potential gradient is proposed. Values of partial oxide ionic conductivity were calculated. It was found that oxygen permeability decreases in the La > Pr > Nd sequence. © 1995 Academic Press, Inc.

1. INTRODUCTION

It appears that rare-earth elements (REE) and strontium cobaltites Ln(Sr)$CoO_{3-\delta}$ are promising materials for high-temperature electrochemical cells of various types due to their high ionic conductivity, compared to such oxide ion conductors as zirconia based solid solutions (1–3). The presence of oxide ionic conductivity in the background of high electronic conductivity for electrode materials leads to a substantial improvement in the electrochemical properties of electrodes, due to the expansion of the electrochemical reaction zone (1, 4). Mixed conducting materials can be used to create oxygen electrochemical membranes, viz., devices designed to produce high-purity oxygen from air, in which the separation of gases occurs by the action of the oxygen chemical potential gradient (2). Nevertheless, the investigation of the parameters of oxide ionic transport on the background of high electronic conductivity is associated with numerous experimental difficulties.

Some data on the ionic conductivity of certain solid solutions based on rare earth elements manganites, ferrites, and cobaltites with perovskite-like structure are adduced in Refs. (1, 5). Regretfully, these data are odd and do not allow us to ascertain the dependence of ionic conductivity on the composition of solid solutions.

In (2, 6, 7) oxygen permeability of the large set of cobaltites was investigated. The oxygen permeability was determined from the quantity of oxygen passing through a specimen attached to a mullite tube by a silver ring and entering the flow of helium. According to these data, oxygen permeability increases with an increase in x in the system $Ln_{1-x}Sr_xCoO_{3-\delta}$ and builds up with the transition La → Gd in solid solutions $Ln_{1-x}Sr_xCoO_{3-\delta}$ (Ln = La, Pr, Nd, Sm, Gd). However, these results are not sufficiently correct on two counts. First, silver is permeable to oxygen and it cannot be used for attachment. Second, both electronic and ionic conductivities of cobaltites depend on the oxygen content in the gaseous phase; consequently, use of air and helium as gases surrounding the opposite surfaces of the specimen under investigation can cause considerable experimental errors due to too large an oxygen pressure drop across a specimen. Comparisons of the data on oxygen permeability obtained at considerable oxygen partial pressure differences across the ceramics can be made only in combination with analysis of the dependence of oxygen permeability on oxygen chemical potential values on both sides of the ceramics. Harnessing of the four-probes method with electronic filters to study partial ionic conductivity of cobaltites (7) is not sufficiently correct because of the absence of any blockade of oxygen exchange between the ceramics under study and the gaseous phase.

It was shown in Ref. (8) by the ^{18}O tracer diffusion method that the values of the oxygen vacancy diffusion coefficient in $LaCoO_{3-\delta}$ exceed the corresponding values for $La_{0.9}Sr_{0.1}CoO_{3-\delta}$ in the temperature range 800 to 1100°C. In Ref. (9) it was found from studies of electrochemical cells with liquid electrolytes that the diffusion coefficient of oxide ions in $Nd_{0.8}Sr_{0.2}CoO_{3-\delta}$ at 25°C (1.4×10^{-11} cm$^2 \times$ s^{-1}) exceeds that in $Nd_{0.5}Sr_{0.5}CoO_{3-\delta}$ (7.6×10^{-14} cm$^2 \times$ s^{-1}). It was found by the gravimetric method (10) that for solid solutions $La_{1-x}Sr_xCoO_{3-\delta}$ ionic conductivity rises in the series (x = 0.65) > (x = 0.5) > (x = 0.2) at temperatures in the range 400–900°C. The only possible disadvantage of the data obtained in (10) is the use of a mathematical apparatus based on the assumptions that the oxide ions' mobility is independent of their chemical potential and that there are no limitations of oxygen transfer caused by adsorption.

0022-4596/95 $12.00

Thus, there are certain discrepancies in the literature data on the parameters of ionic transport in $Ln(Sr)CoO_{3-\delta}$ solid solutions.

The purpose of the present work is to investigate the physicochemical properties of $Ln_{1-x}Sr_xCoO_{3-\delta}$ and the oxide ion transference parameters of these solid solutions. When studying oxygen permeability of cobaltites, we tried to avoid the failings associated with the use of fixed compositions of gases on different sides of the specimen, with too large a difference in the oxygen partial pressure in given gas mixtures, with the use of only one value of this difference, and with failure to take into account the diffusion boundary conditions. Such flaws are typical in investigations of oxygen permeability and can be found in many works (e.g., Refs. (2, 5, 6, 11)). In the present work the specimen being investigated was covered by the glass to achieve the linear diffusion of oxide ions in the maximum extension. Oxygen partial pressure at one side of the specimen was varied in a wide range by an electrochemical pump and controlled by an oxygen sensor. The reproducibility of the oxygen permeability values was verified only in connection with specific values of oxygen partial pressure on both sides of the specimen under investigation. One of the tasks of our work was the elaboration of the model of the dependence of cobaltites' oxygen permeability on oxygen partial pressure.

2. EXPERIMENTAL

The synthesis of $La_{1-x}Sr_xCoO_{3-\delta}$ (x = 0.0–1.0) and $Ln_{1-x}Sr_xCoO_{3-\delta}$ (Ln = Pr, Nd; x = 0.0–0.5) polycrystalline samples was carried out by standard ceramics technology from oxides, nitrates, and carbonates at temperatures of 1370–1570 K for 15–35 hr in air. During the process of synthesis multiple powder milling was used. The X-ray diffraction patterns were taken with a DRON-3M diffractometer using Cu$K\alpha$ and Co$K\alpha$ radiation (Ni and Fe filters). The error in the crystalline lattice constants was ±0.0001 nm. Quantitative analysis of cations and evaluation of oxygen content was carried out by the X-ray fluorescence analysis (XFA) method on "Microscan-5" and scanning electron microscope "Nanolab-7" with the micro X-ray fluorescence spectrometer SR-860-2.

Ceramic samples were pressed from powders of synthesized cobaltites under pressures of 300–600 MPa, in the shape of bars (4 × 4 × 30 mm) and tablets (diameter 15 or 28 mm, thickness 3–4 mm). Ceramics were calcined at 1470–1670 K for 20–35 hr. The ceramic samples' density (d_{exp}) was 80–95% of the theoretical density. Obtained ceramics were tested for gas-tightness (absence of open porosity) using a spirit solution of "Sudan" dye-stuff and by means of the helium-vacuum method with the leak-detector GTI-3.

The methods of synthesizing cobaltites, making ceramics, and investigating crystal structure and composition are described in detail in our previous papers (12, 13).

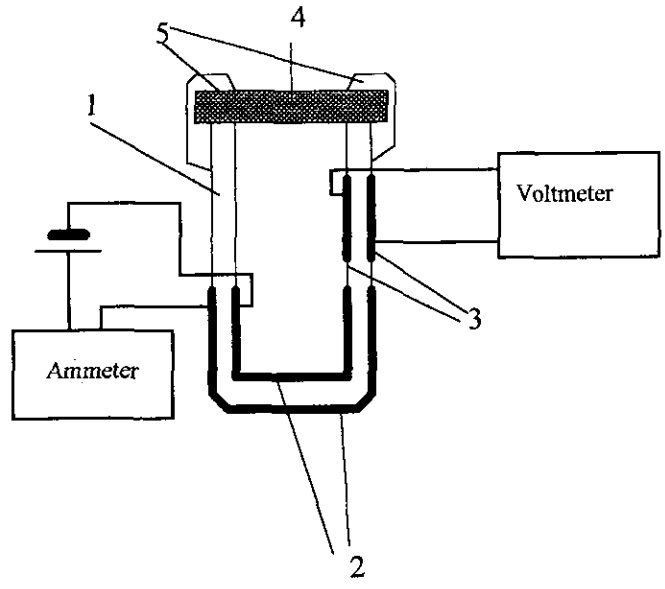

FIG. 1. Electrochemical cell for oxygen permeability measurements: 1, solid electrolyte; 2, electrodes of the oxygen pump; 3, electrodes of the oxygen sensor; 4, measured sample; 5, high-temperature glass.

The electrical conductivity was measured by the four-probe DC method in air at temperatures from 300 to 1100 K and isothermally in different atmospheres with oxygen partial pressures from 1×10^{-5} to 0.21×10^5 Pa. The various oxygen partial pressures in the measuring cell were obtained by means of a solid electrolyte oxygen pump and were controlled by the gas analyzer "Zirkon-M." Relative error of conductivity measurement did not exceed 2%.

Oxygen permeability measurements were carried out with the help of an electrochemical cell outfitted with an oxygen pump and sensor (Fig. 1). The investigation procedure is described in detail in previous papers (12, 13). Oxygen permeability was determined subject to the condition that the flow of the oxygen coming to the cell through a tightly glued sample due to the ionic conductivity of cobaltite should be equal to the flow of the oxygen removed from the cell by the oxygen pump. Oxygen permeability was measured over the temperature range from 950 to 1370 K by the difference of the partial pressures of oxygen in the internal and external spaces of the measuring cell between 1×10^4 and 1×10^3 Pa. The time for the cell to reach a steady state was 0.5 to 6 hr. Measurements were made on ceramics whose gas tightness was determined previously by the vacuum-helium method using a GTI-3 detector.

The oxygen permeability of the cobaltites, $J(O_2)$ (mol/s × cm), was calculated from the formula (14)

$$J(O_2) = \frac{RT}{16F^2} \times t_o \times (1 - t_o) \times \overline{\sigma} = \frac{RTd}{16F^2S} \times \frac{I}{E}, \quad [1]$$

where t_o is the oxide ionic transference number equal to the ratio between the oxide ionic conductivity and the specific conductivity of the sample. $\bar{\sigma}$ is the mean specific electrical conductivity over the interval of partial oxygen pressures from p_1 to p_2. d and S are the thickness and effective area of the test sample, respectively. I is the intensity of the current through the measuring-cell oxygen pump, which evacuates oxygen from the internal to the external space. E is the e.m.f. of the oxygen sensor of the cell,

$$E = \frac{RT}{4F} \ln \frac{p_2}{p_1}, \quad [2]$$

with p_1 and p_2 being the partial oxygen pressures in the internal and the external space of the measuring cell. Since both the electronic and the oxide ionic conductivity of the oxides depend on the oxygen pressure, the quantity $J(O_2)$ can characterize a material only in combination with the corresponding p_1 and p_2 or E values.

The variance of reproducibility for the oxygen permeability of cobaltites did not exceed 5% with respect to the measured value.

The effective activation energy of oxide ionic conductivity was calculated using the regression model

$$\sigma_o = A_0 \frac{1}{T} \exp\left[-\frac{E_a}{RT}\right], \quad [3]$$

where E_a is the effective activation energy and A_0 is the preexponential factor. The ionic conductivity (σ_o) and oxide ionic transference numbers (t_o) were calculated using the equations

$$t_o \times (1 - t_o) \times \bar{\sigma} = \frac{d}{S} \times \frac{dI}{dE} \quad [4]$$

$$\sigma_o = t_o \times \bar{\sigma}. \quad [5]$$

For the calculation of oxide ionic conductivity we used experimental data corresponding to values of the correlation coefficient of the linear dependence $I = f(E)$ that were not less than 0.995.

3. RESULTS AND DISCUSSION

X-ray diffraction testing results of synthesized samples $La_{1-x}Sr_xCoO_{3-\delta}$ (x = 0–0.7) and $Ln_{1-x}Sr_xCoO_{3-\delta}$ (Ln = Pr, Nd; x = 0.0–0.5) showed that formation of the series of perovskite-type solid solutions with cubic, orthorhombic, or rhombohedric structures took place in the investi-

TABLE 1
Properties of $Ln_{1-x}Sr_xCoO_{3-\delta}$ Ceramics

Ln	x	Structure[a]	a (nm)	b (nm)	c (nm)	α (°)	d_{ren}[b] (kg/m^3)	d_{exp}[b] (kg/m^3)
La	0.0	R	0.5388			60.80	7214	6100
	0.1	R	0.5390			60.62	7113	6020
	0.2	R	0.5407			60.56	6907	5840
	0.3	R	0.5411			60.44	6762	5590
	0.4	R	0.5414			60.32	6618	5410
	0.5	R	0.5418			60.24	6467	5360
	0.6	C	0.3830				6359	5250
	0.7	C	0.3834				6188	5170
Pr	0	C	0.7561				7616	6390
	0.1	C	0.7587				7375	6360
	0.2	C	0.7595				7190	5950
	0.3	C	0.7600				7015	5790
	0.4	C	0.7606				6838	5660
	0.5	C	0.7614				6656	5500
Nd	0	C	0.7548				7709	6600
	0.1	C	0.7562				7493	6680
	0.2	R	0.5340			59.40	7456	6170
	0.3	R	0.5363			60.22	7050	6000
	0.4	O	0.5354	0.5333	0.7644		6909	5880
	0.5	O	0.5352	0.5408	0.7614		6671	5730

[a] C denotes cubic structure of perovskite and R and O denote perovskite structure having rhombohedric and orthorhombic distortions, respectively.

[b] d_{ren} and d_{exp} are the theoretical and experimental density.

TABLE 2
Transference Parameters of $Ln_{1-x}Sr_xCoO_{3-\delta}$

Ln	x	TRC × 10^4 (K^{-1}) 300–700 K	E_a (kJ/mol) T(K)	E_a (kJ/mol) Value	t_O[a]
La	0.0	—	1100–1250	16 ± 2	0.0007
	0.2	1.9 ± 0.2	1100–1250	25 ± 7	0.0003
	0.3	7.5 ± 1.0	—	—	—
	0.4	6.4 ± 0.3	1100–1250	33 ± 6	0.0001
	0.5	10.3 ± 0.3	1100–1200	29 ± 5	0.0005
	0.6	10.6 ± 0.2	—	—	—
	0.7	11.4 ± 0.5	1100–1250	23 ± 7	0.0012
	0.8	—	1150–1300	17 ± 3	0.0008
Pr	0	—	970–1200	49 ± 5	0.0002
	0.1	—	970–1120	46 ± 4	0.0002
	0.2	—	970–1200	47 ± 4	0.0002
	0.3	0.9 ± 0.2	970–1200	54 ± 3	0.0001
	0.4	8.3 ± 0.5	970–1200	51 ± 5	0.0001
	0.5	10.7 ± 2.2	—	—	—
Nd	0.2	—	970–1200	48 ± 7	0.0001
	0.3	1.3 ± 0.3	970–1200	51 ± 3	0.0001
	0.4	6.0 ± 0.4	970–1200	43 ± 5	0.0001
	0.5	8.6 ± 0.6	—	—	—

[a] t_O is the oxide ion transference number for $La_{1-x}Sr_xCoO_{3-\delta}$ at 1105 ± 5 K and $Ln_{1-x}Sr_xCoO_{3-\delta}$ (Ln = Pr, Nd) at 1115 ± 5 K.

gated region. Thermodynamic stability of cobaltites was confirmed by DTA methods, by high-temperature X-ray diffraction analysis, and also by maintenance of phase composition and structure in a long annealing session (up to 100 hr) in the temperature region from 870 to 1270 K. The type of perovskite structure (Table 1) is mostly dependent on synthesis conditions (temperature, atmosphere, heating, and cooling rate) and oxygen nonstoichiometry (15). Only the structures of $La_{1-x}Sr_xCoO_{3-\delta}$ (x = 0–0.7) solid solutions are in agreement with the tolerance factor t calculation (according to (15, 16)). Formation of a cubic structure with doubling of the unit cell parameter is connected with oxide ion substructure regulation for $Ln_{1-x}Sr_xCoO_{3-\delta}$ (Ln = Pr, Nd). Superstructure formation in the oxide ion sublattice gives no new reflections of X-ray patterns. Calculated values of the elementary cell volume rise when x increases because the ion radius of the Sr^{2+} cation is greater than that of Ln^{3+}.

The results of the XFA showed that the deviations of cationic composition in each sublattice of the perovskite structure from the formula data have not exceeded 2%. The overall impurity concentration consisted of not more than 0.5 at.%.

The results of cobaltites specific conductivity investigations were published earlier (13). Temperature dependencies of the electrical conductivity of $Ln_{1-x}Sr_xCoO_{3-\delta}$ are in agreement with the literature data (17, 18). The doping by strontium leads to a sharp conductivity increase and a transition to a metallic type of conduction at $x > 0.2$. Temperature resistance coefficients (TRC) of the investigated materials are given in Table 2. TRC values were calculated using the equation

$$\rho = \rho_0 \times (1 + \beta \times T), \qquad [6]$$

where β is TRC, ρ is the specific resistance, and ρ_0 is the specific resistance at 298 K.

The conductivity of cobaltites does not depend on the oxygen partial pressure at temperatures lower than 700 K (Fig. 2). The reversible conductance decrease with the oxygen partial pressure drop was observed at $T > 900$ K. The variation of conductivity increases with increasing strontium concentration and increasing temperature. Because the electronic component of the conductivity is far above the ionic one, the cobaltites' specific conductivity as a function of the oxygen content in the gaseous phase may be quite correctly described using the empirical model

$$\sigma = b_1 \times p^n + b_2, \qquad [7]$$

where p (atm) is the oxygen partial pressure. Some results of the regression analysis of the oxygen pressure dependen-

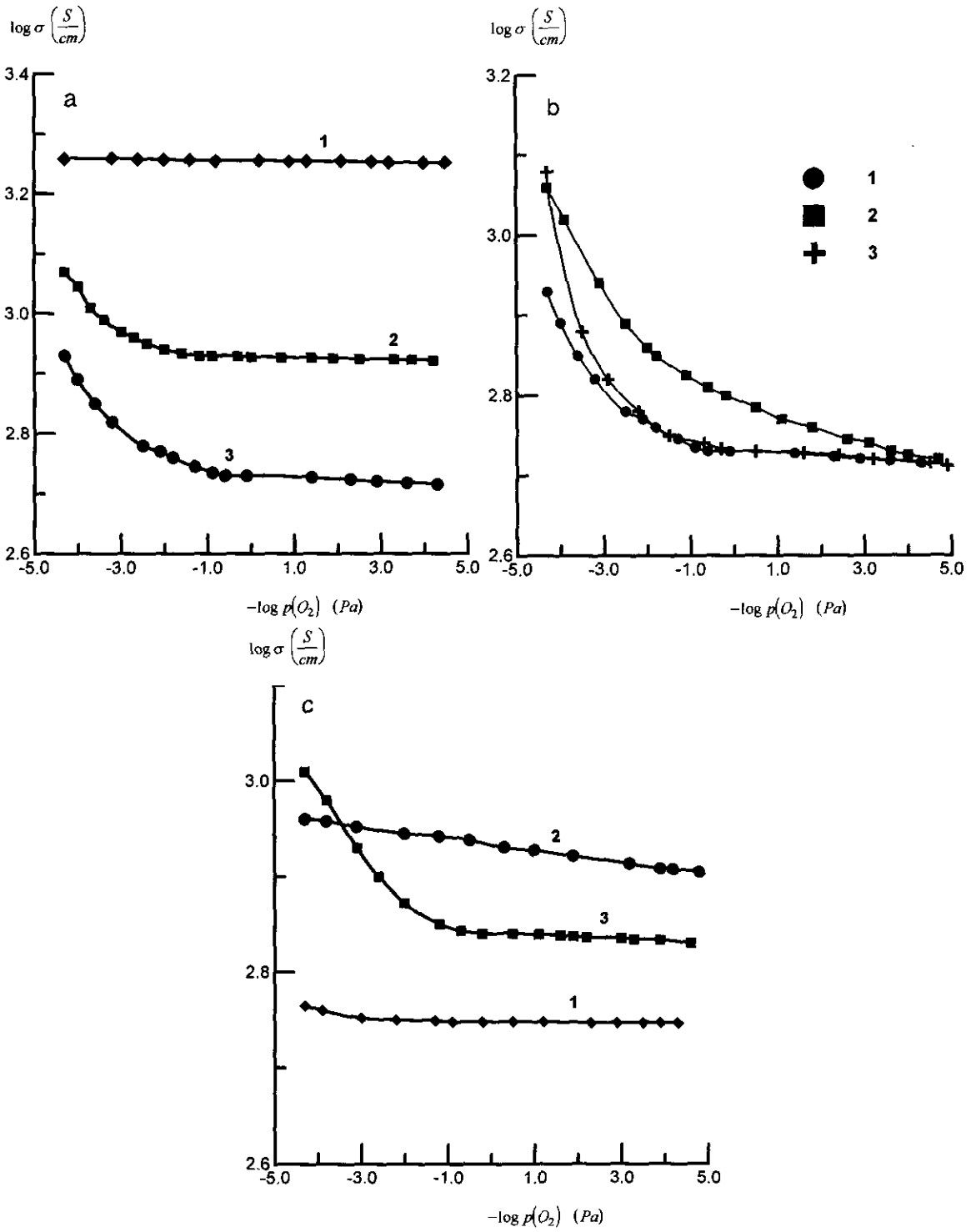

FIG. 2. $p(O_2)$ dependence of conductivity for (a) $La_{0.5}Sr_{0.5}CoO_{3-\delta}$ at 670 (1), 970 (2), and 1070 K (3); (b) $Ln_{0.5}Sr_{0.5}CoO_{3-\delta}$ at 1070 K for Ln = La (1), Pr (2), and Nd (3); (c) $Nd_{1-x}Sr_xCoO_{3-\delta}$ at 1070 K for x = 0 (1), 0.1 (2), and 0.3 (3).

cies of the cobaltites' conductivity according to the model Eq. [7] were published in (19).

The Ln^{3+} ion radius dependence of electrical properties of REE cobaltites can be described by the Raccah and Goodenough model (20). Ion radius diminution in lanthanide's sequence causes strengthening of "Ln cation–oxide anion" interaction and hence the orbitals' overlap integral decreases for cobalt and oxide ion. The value of $Ln_{1-x}Sr_xCoO_{3-\delta}$ electronic conductivity caused by the Co—O—Co bond covalence degree is reduced as the REE number is increased. The most characteristic type of electronic conductivity dependence on the lanthanide ion radius can be observed at T = 600–700 K. The cobaltites conductivity depends on the cobalt ion content in high oxidation states at lower temperatures (T < 500 K). The cobalt ion state in this temperature range is determined by oxygen nonstoichiometry and sample history. The temperature increase leads to the conductivity type changing to metallic and the $Ln_{1-x}Sr_xCoO_{3-\delta}$ conductivity values becoming more close to one another. Strontium doping also leads to the fact that $Ln_{1-x}Sr_xCoO_{3-\delta}$ the specific conductivity of solid solutions becomes more close to one another. Electronic conductivity of $Ln_{1-x}Sr_xCoO_{3-\delta}$ at 600 K decreases by a factor of 300 for the La–Gd sequence (Fig. 3). Data on $GdCoO_{3-\delta}$ was published earlier (13, 21).

Perovskite-like oxides based on lanthanum cobaltite are characterized by a vacancy mechanism of oxide ionic transport (e.g., (8)). Assuming that at a given gradient of the oxygen chemical potential the phase composition of oxides is constant, the partial ionic and electronic conductivities under isothermal conditions can be expressed as (22)

$$\sigma_o = K_o \times c_o \times [V_o] \times N \qquad [8]$$

$$\sigma_e = K_e \times h \times \frac{N}{3}, \qquad [9]$$

where $[V_o]$ and c_o stand for the fractions of vacant and occupied sites in the oxide ion sublattice, respectively; N is the concentration of oxide ion sites; ($h \times N/3$) is the concentration of holes (h is a relative concentration of holes); and K_o and K_e are constants. In accordance with the equation for the oxygen exchange,

$$\frac{1}{2}O_2 + V_o^{\bullet\bullet} \Leftrightarrow O^{\times} + 2h^{\bullet}$$

(with $h^{\bullet}$ being an electron hole), the concentrations of oxide ions and vacancies, in terms of the point defect model, are related by the expressions

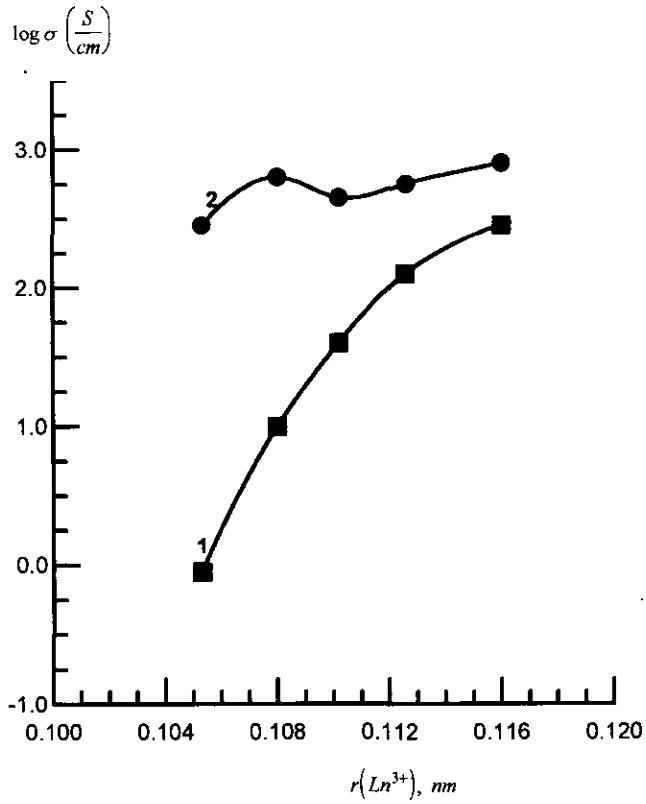

FIG. 3. Lanthanide ion radius dependence on conductivity for $LnCoO_{3-\delta}$ at 600 (1) and 1000 K (2).

$$K_p = \frac{\sqrt{p} \times [V_o]}{c_o \times h^2} \qquad [10]$$

$$K_g = \frac{h}{3} + 2[V_o] \qquad [11]$$

$$[V_o] + c_o = 1, \qquad [12]$$

where K_p and K_g are constants and p is the partial oxygen pressure. The density of the molecular oxygen flow passing through the ceramic under the action of the chemical potential difference can be expressed as

$$j = K_m \int_{c_1}^{c_2} \frac{\sigma_O \times \sigma_h}{\sigma_O + \sigma_h} \times \frac{d(\ln p)}{dc_O} dc_O \qquad [13]$$

with $K_m = (RT/16F^2d)$, where c_1 and c_2 are the values of c_o in the surface layers of cobaltite ceramic.

Substituting the solution of the set of Eqs. [8]–[12] into Eq. [13] yields, upon integrating, the expression for the density of the molecular oxygen flow through the oxide ceramic material

$$j = 6K_mK_e\left[\frac{12K_e - K_o}{K_o\lambda}\left(\begin{array}{l}(\lambda + 6K_e + K_o(K_g - 1))\ln\left[\dfrac{2K_oc_2 - 6K_e - K_o - \lambda}{2K_oc_1 - 6K_e - K_o - \lambda}\right] \\ + (\lambda - 6K_e - K_o(K_g - 1))\ln\left[\dfrac{2K_oc_2 - 6K_e - K_o + \lambda}{2K_oc_1 - 6K_e - K_o + \lambda}\right]\end{array}\right) + 4(c_2 - c_1)\right], \quad [14]$$

where $\lambda = \sqrt{36K_e^2 + 12K_eK_gK_o - 12K_eK_o + K_o^2}$.
Since $\sigma_h \gg \sigma_o$, we may assume that

$$j = K_m\int_{c_1}^{c_2}\sigma_O\frac{d(\ln p)}{dc_O}dc_O. \quad [15]$$

In this case the solution simplifies to

$$j = K_o^{\bullet}N\left[K_g(2 - K_g)\ln\left(\frac{2c_2 + K_g - 2}{2c_1 + K_g - 2}\right) - 2(c_2^2 - c_1^2) + 2(K_g + 1)(c_2 - c_1)\right], \quad [16]$$

where, in accordance with the phenomenological theory of ionic transport (22),

$$K_o^{\bullet} = \gamma \times v_o \times \frac{r^2}{4d} \times \exp\left[-\frac{U_0}{RT}\right],$$

with γ being the geometrical factor, v_o and r the mean oscillation frequency and the elementary jump length of oxide ions, and U_o the free energy of migration.

A particular case of Eq. [16] is the formula for the density of the oxygen flow through $Ln_{1-x}Sr_xCoO_{3-\delta}$ ceramics. In this case one of the conditions for the crystal to be electroneutral, Eq. [11], can be written as

$$\frac{h}{3} + 2[V_o] = \frac{x}{3}$$

or

$$K_g = \frac{x}{3}. \quad [17]$$

The expression for the density of the oxygen flow can be presented as

$$j = K_o^{\bullet}N\left[\frac{x}{3}\left(2 - \frac{x}{3}\right)\ln\left(\frac{6c_2 + x - 6}{6c_1 + x - 6}\right) - 2(c_2^2 - c_1^2) + 2\left(\frac{x}{3} + 1\right)(c_2 - c_1)\right]. \quad [18]$$

The dependencies of the oxygen permeability of $Ln(Sr)CoO_{3-\delta}$ ceramics on the oxygen partial pressure ratio inside and outside the measuring cell are shown in Fig. 4. The nonlinear dependence of $J(O_2) = f(E)$ indicates the inadequacy of Eq. [1] for the description of the oxygen transport processes in the cobaltites. Such a fact can be conditioned either by the adsorption limitation of oxygen transport or by the partial conductivities dependence from oxygen pressure.

The regression analysis of the data on oxygen permeability was performed by the least-squares method using a positive definite secant formula (BGFS-formula) to minimize the adequacy dispersion (23). Statistical parameters of nonlinear models were evaluated by the techniques proposed in (24).

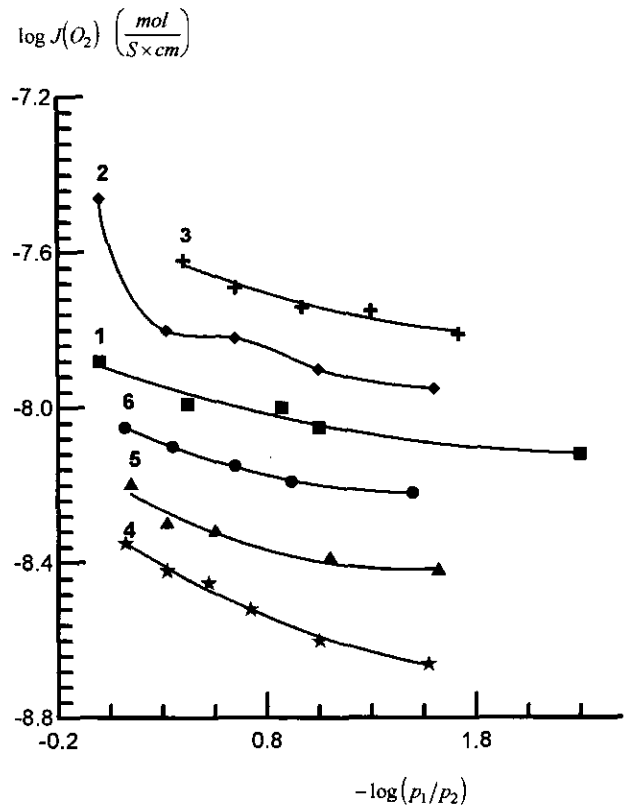

FIG. 4. Representative oxygen permeability of $Pr_{0.9}Sr_{0.1}CoO_{3-\delta}$ (1–3) and $Nd_{0.7}Sr_{0.3}CoO_{3-\delta}$ (4–6) solid solutions dependence on the oxygen pressure ratio inside and outside the cell at 970 (1, 4); 1065 (2, 5); and 1165 K (3, 6).

In addition to Eq. [14] and Eq. [18], the solutions of the systems of equations that include Wagner's law, Langmuir's or Frehinlich's adsorption isotherms, and the models proposed in (14, 19) were used as regression models.

The most adequate description of the experimental data on oxygen permeability of $Ln(Sr)CoO_{3-\delta}$ ceramics is provided by the model derived from Eq. [18] using the adsorption isotherm

$$c_i = \frac{K_{sorb} \times p_i^m}{1 + K_{sorb} \times p_i^m}, \qquad [19]$$

where K_{sorb} and m are constants.

The most adequate regression model can be obtained by substituting Eq. [19] into Eq. [18],

$$j = \frac{k_1}{d}\left[\frac{x}{3} \times \left(2 - \frac{x}{3}\right) \times \ln\frac{2c_2 + \frac{x}{3} - 2}{2c_1 + \frac{x}{3} - 2} - 2(c_2^2 - c_1^2) + 2\left(\frac{x}{3} + 1\right) \times (c_2 - c_1)\right] + k_3, \qquad [20]$$

where $c_i = (k_2^2 \times p_i^m)/(1 + k_2^2 \times p_i^m)$, $k_1 = K_o^{\bullet} \times N \times d$, $k_2 = \sqrt{K_{sorb}}$, and k_i and m are regression parameters. The parameter of k_3 corresponds to the error of the oxygen flow measurements.

The fitting results obtained using this model for some composition of $Ln(Sr)CoO_{3-\delta}$ are given in Table 3. With this model, the calculation error slightly exceeds the instrumental error.

The geometrical calculation of the distance between cations in the most probable anion jump direction for REE and strontium cobaltites confirms that anion transfer channel size decreases in the La → Nd sequence. Nevertheless the ionic conductivity value is to large degree defined by the interaction of the O^{2-} ion with the nearest neighboring cation (4 A ions and 2 B ions of the ABO_3 perovskite structure). From this point of view the lanthanide ion radius decrease causes further weakening of the B–O bond and the A–O bond energy increase which can lead to an oxide ionic conductivity decrease. B^{4+} ion existence means that the B–O bond covalence is rising. In this case ionic conductivity decreases.

The ionic conductivity variations in $Ln_{1-x}Sr_xCoO_{3-\delta}$ systems (Fig. 5) are in agreement with the previous conclusion. The ionic conductivity decreases as x increases at x values between 0 and 0.4. Then oxide ionic conductivity increases with the x increase from 0.5 to 0.7. Most probably, the discussed change of the ionic conductivity is due to the corresponding variation of the concentration of the oxygen vacancy and Co^{4+} ions (14). Ionic conductivity decreases with an x increase from 0.8 to 1.0 because these complex oxides are not single phase compounds. The value of ionic conductivity diminishes in the La > Pr > Nd sequence. The values of effective activation energy for oxide ion conductivity derived from the Arrhenius law and the oxide ion transference numbers are given in Table 2.

TABLE 3
Parameters of the Regression Model (Eq. [20]) for the Oxygen Flow Density through $Ln_{1-x}Sr_xCoO_{3-\delta}$ Ceramics

Ln	x	T (K)	$k_1 \times 10^6$	k_2	$k_3 \times 10^7$	m	ρ^a	s^b (%)
La	0.2	1102	16 ± 1	1.8 ± 0.1	[c]	0.80	0.0997	2.37
	0.5	1176	20.9 ± 0.6	1.38 ± 0.08	[c]	1.00	0.9998	0.50
	0.7	1103	25 ± 1	2.38 ± 0.09	15 ± 3	1.20	0.9991	0.83
	0.7	1175	32 ± 2	1.8 ± 0.1	[c]	1.00	0.998	1.20
	0.8	1102	9.78 ± 0.01	10.42 ± 0.01	2.78 ± 0.01	2.7	0.9999	0.01
Pr	0.9	971	13.6 ± 0.4	0.76 ± 0.02	[c]	0.40	0.9999	0.35
	0.9	1112	18 ± 3	0.85 ± 0.23	[c]	0.50	0.996	1.79
	0.7	970	7.64 ± 0.07	0.87 ± 0.01	[c]	0.30	0.9999	0.24
	0.7	1116	8.0 ± 0.3	4.2 ± 0.2	3.4 ± 0.3	1.00	0.998	1.06
	0.6	970	12 ± 1	0.94 ± 0.08	[c]	0.20	0.997	1.97
	0.6	1116	20 ± 2	0.7 ± 0.2	[c]	0.25	0.991	3.41
Nd	0.6	1105	6.5 ± 0.7	0.7 ± 2	[c]	0.30	0.9991	0.88

[a] ρ is the correlation coefficient.
[b] s is the relative error of the model.
[c] The parameter is nonsignificant.

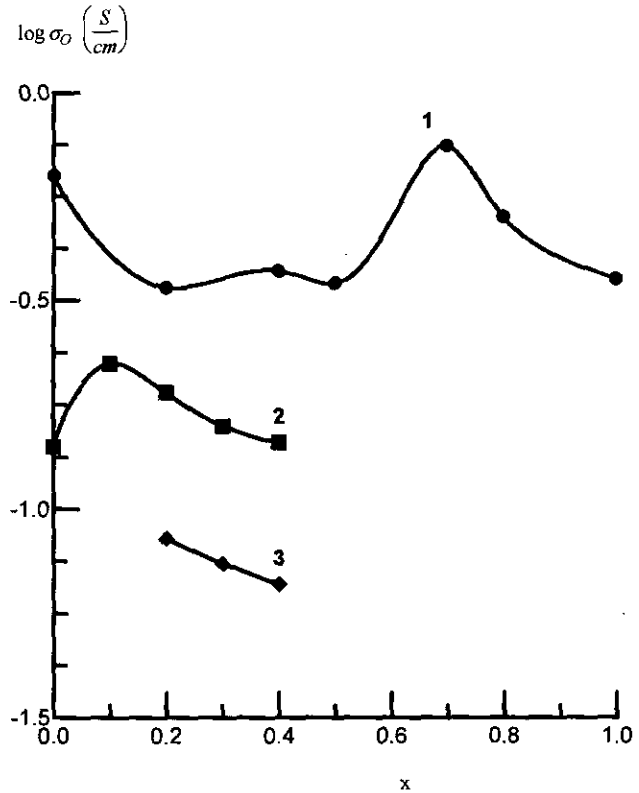

FIG. 5. Oxide ionic conductivity dependence on the strontium content for $La_{1-x}Sr_xCoO_{3-\delta}$ (1) at 1105 ± 5 K, $Pr_{1-x}Sr_xCoO_{3-\delta}$ (2), and $Nd_{1-x}Sr_xCoO_{3-\delta}$ (3) at 1115 ± 4 K.

REFERENCES

1. T. Takahashi and H. Iwahara, *in* "Reports of Special Project Research," p. 727. Grant in Aid of Scientific Research of the Ministry of Education, Science and Culture, Japan, 1980.
2. Y. Teraoka, H.-M. Zhang, S. Furukawa, and N. Yamazoe, *Chem. Lett. Chem. Soc. Jpn.* **11,** 1743 (1985).
3. P. Shuk, A. Vecher, V. Kharton, L. Tikhonova, H.-D. Wiemhoefer, U. Guth, and W. Goepel, *Sensors and Actuators.B* **15**(6), 401 (1993).
4. M. V. Perfilyev, A. K. Demin, B. L. Kuzin, and A. S. Lipilin, "High Temperature Electrolysis of Gases." Nauka, Moscow, 1988. [In Russian]
5. S. Carter, A. Selcuk, R. J. Chater, J. Kajda, J. A. Kilner, and B. C. H. Steele, *Solid State Ionics* **53**(56), 597 (1992).
6. Y. Teraoka, T. Nobunaga, and N. Yamazoe, *Chem. Lett. Chem. Soc. Jpn.* **6,** 503 (1988).
7. Y. Teraoka, H.-M. Zhang, K. Okamoto, and N. Yamazoe, *Mater. Res. Bull.* **23,** 51 (1988).
8. T. Ishigaki, S. Yamauchi, K. Kishio, J. Mizusaki, and K. Fueki, *J. Solid State Chem.* **73,** 179 (1988).
9. T. Kudo, H. Obayashi, and T. Gejo, *J. Electrochem. Soc.* **122,** 159 (1975).
10. S. Sekido, H. Tachibana, Y. Yamamura, and T. Kambara, *Solid State Ionics* **37,** 253 (1990).
11. H. J. M. Bouwmeester, H. Kruidhof, A. J. Burgraaf, and P. J. Gellings, *Mater. Sci. Forum* **76,** 165 (1991).
12. V. V. Kharton, E. N. Naumovich, P. P. Shuk, A. K. Demin, and A. V. Nikolaev, *Electrochemistry* **28,** 1693 (1992). [In Russian]
13. V. V. Kharton, P. P. Shuk, A. K. Demin, A. V. Nikolaev, A. A. Tonoyan, and A. A. Vecher, *in* "Ionics of Solid State" (M. V. Perfilyev, Ed.), p. 3. Nauka, Ekaterinburg, 1993. [In Russian]
14. H.-H. Moebius, *Ext. Abstr. 37th Meet. Int. Soc. Electrochem.* **1,** 136 (1986).
15. G. J. McCarthy, *Rare Earth Mod. Sci. Technol.*, 189 (1978).
16. H. Ohbayashi, T. Kudo, and T. Gejo, *Jpn. J. Appl. Phys.* **13,** 1 (1974).
17. J. Schroeder, *Z. Naturforsch.* **176,** 346 (1962).
18. S. Jacobs, R. Hartung, H.-H. Moebius, and M. Wilke, *Rev. Chim. Miner.* **17,** 283 (1980).
19. V. V. Kharton, E. N. Naumovich, A. V. Nikolaev, and A. A. Vecher, *Lett. Belarus Acad. Sci. Ser. Chem. Sci.* **3,** 53 (1993). [In Russian]
20. N. Ramadass, *Mater. Sci. Eng.* **36,** 189 (1978).
21. V. V. Kharton, P. P. Shuk, A. A. Tonoyan, and A. A. Vecher, *Lett. Belarus Acad. Sci. Ser. Chem. Sci.* **3,** 35 (1991). [In Russian]
22. V. N. Chebotin, "Chemical Diffusion in Solid State." Nauka, Moscow, 1989. [In Russian]
23. J. E. Dennis, Jr., and R. B. Schnabel, "Numerical Methods for Unconstrained Optimisation and Non-linear Equations." Prentice-Hall, New York, 1983.
24. N. R. Draper and H. Smith, "Applied Regression Analysis." Wiley, New York, 1981.